Article citation info:
CHUDZIK A, WARDA B. Effect of radial internal clearance on the fatigue life of the radial cylindrical roller bearing. Eksploatacja i Niezawodnosc – Maintenance and Reliability 2019; 21 (2): 211–219, http://dx.doi.org/10.17531/ein.2019.2.4.

Agnieszka CHUDZIK
Bogdan WARDA

EFFECT OF RADIAL INTERNAL CLEARANCE ON THE FATIGUE LIFE OF THE RADIAL CYLINDRICAL ROLLER BEARING

WPŁYW WEWNĘTRZNEGO LUZU PROMIENIOWEGO NA TRWAŁOŚĆ ZMĘCZENIOWĄ PROMIENIOWEGO ŁOŻYSKA WALCOWEGO*

The paper presents result of the research on influence of internal radial clearance in radial cylindrical roller bearing on its fatigue durability. By solving the Boussinesq problem for the elastic half-space and finite elements method, stress distributions were determined, necessary to estimate predicted fatigue life of the bearing. The calculations took into account geometrical parameters of the bearing: its radial clearance and shape of rolling parts. Predicted radical clearance was computed by using the Lundberg and Palmgren model. ANSYS program allowed to introduce the analysis of von Mises stress distribution in any plane of cooperating components. The outcome revealed, radial cylindrical roller bearing will have highest endurance with slight radial clearance.

Keywords**:** *rolling bearing; stress distribution; fatigue life; finite element method; radial clearance.*

W pracy przedstawiono wyniki badań wpływu wewnętrznego luzu promieniowego w promieniowym łożysku walcowym na jego prognozowaną trwałość zmęczeniową. Wykorzystując zagadnienie Boussinesqa dla półprzestrzeni sprężystej i metodę elementów skończonych, określono rozkłady naprężeń podpowierzchniowych niezbędne do oszacowania prognozowanej trwałości zmęczeniowej łożyska. W obliczeniach uwzględniono geometryczne parametry łożyska: jego luz promieniowy i kształt części tocznych. Do określenia wartości luzu promieniowego wykorzystano model Lundberga i Palmgrena. Zastosowanie programu ANSYS pozwoliło na przeprowadzenie analizy rozkładu naprężeń von Misesa w dowolnej płaszczyźnie współpracujących ze sobą elementów tocznych łożyska. Analiza obliczeń wykazała, że promieniowe łożysko walcowe będzie miało najwyższą wytrzymałość z niewielkim luzem promieniowym.

Słowa kluczowe*: łożysko walcowe, rozkład naprężeń, trwałość zmęczeniowa, metoda elementów skończonych, luz promieniowy***.**

Nomenclature

A	material constant
B	bearing width
C	basic dynamic load rating
D	bearing outside diameter
D_r	roller diameter
E	Young's modulus
F_r	radial load of the bearing
INT	integer function
L	fatigue life
L_r	roller length
Q_r	resultant normal force in the roller-main race contact
S_t	Stribeck's constant
U_z	local displacement inside the bearing elements
Z	depth of occurrence of maximal von Mises stresses along the *x* axis
Z_r	number of rollers in the bearing
b	half width of the contact
c	exponent in the equation determining the survival probability
d	bearing bore diameter
d_{bi}	diameter of the inner ring raceway
d_{bo}	diameter of the outer ring raceway
e	Weibull slope
g	radial clearance in the bearing
h	exponent in the equation determining the survival probability
i	inner raceway
j	number of roller
l	length of the roller-main race contact area
o	outer raceway
n	number of pairs of loaded items
r_b	radius of the main race
r_c	roller chamfer
u	number of load cycles per one revolution
δ_{max}	maximum elastic deformation
δ_c	total displacement of the bearing axis
ν	Poisson's constant
σ	maximal von Mises stress occurring along the *x* axis

(*) Tekst artykułu w polskiej wersji językowej dostępny w elektronicznym wydaniu kwartalnika na stronie ***www.ein.org.pl***

ϕ survival probability of the bearing
ψ angle measured along the bearing circumference
ψ_j angle between rollers
ψ_ε angle of the loaded zone

1. Introduction

Researches of rolling bearing and forecasting their fatigue life were carried out over many years. The deciding factors, having direct influence on approximations of fatigue life are the phenomena occurring between roller elements and raceways. Analytical computational methods of fatigue life does not allow to consider many factors, e.g.:

- bearings radial clearance;
- shape of rolling element generators;
- bearing ring misalignment;
- axial load of radial cylindrical roller bearing.

Moreover analytical computational methods does not allow to predict result of inaccuracy of rolling bearing elements production, insufficient rigidness of development and deflection of bearing roller. FEM become commonly used tool in many domains of science and technology. Applying it allows to introduce parameters, which in analytical computations were unavailable until now. The goal of the numerical and analytical analysis was to research the phenomena occurring in rolling elements single interface and bearing's raceways. Due to the complexity of the researched model, to numerical computations author used solid model of bearing section from half of a bearing and relevant fragments of both rings.

Contact surface of cooperating elements with non-flat contact areas of all devices is very small. With relatively small loading forces, considerable surface pressures are generated causing subsurface stresses. Subsurface stresses have a significant effect on the durability of structural elements. This kind of problem occurs in gearing and all kinds of rolling bearings. H. Hertz [7] initialled the research on the contact surface under pressure. He presented general contact solution of a two elastic bodies to expose radial load. This paper was the basis for Lundberg's research [14], who provided an analytical solution of the model in which a cylinder is compressed between two planes. In 1907, Stribeck [23] showed that the bearing's external load is carried by a part of the rolling element and the load on the individual rolling element depends on their position and the bearing's internal clearance. The greater the clearance between rolling elements, the smaller the number of rollers that carry the load and the greater the force will act on the roller lying on the line of action of external force. Stribeck [23] stated, that the value of the force acting on the roller in case of zero internal clearance bearings is 4.37 of the mean roller bearing load . He suggested, that the value of this force was 5 times the average force, for a bearing with non-zero internal load. Palmgren [17] proposed that for a roller bearing with zero inner clearance, this value should be 4.08. For the other bearings with typical internal clearance, including cylindrical roller bearings, it should be 5. This constant was called the Stribeck's constant.

Rolling bearings are commonly used in engineering designs. These are elements which align the axis of the shaft that carry both radial and axial loads. Rolling bearing is required to sustain long working hours and have high durability. For many years, rolling bearings have been the object of interest for researchers who try to determine rolling bearing's working time up to their failure for various working conditions. That is, to determine the time of failure-free operation of a bearing. Lundberg and Palmgren [15, 16] initiated studies of the effect of internal load on durability of rolling bearings. There were also comprehensive research of different types of surface contact [9], including proposals for calculating the load distribution for rolling elements in various kinds of bearings [2, 3, 4, 5, 6, 8]. The simulations carried out on numerical models of bearings are a convenient and affordable tool for carrying out such tests. For this purpose, numerical models of bearings are built, loaded with external forces (transverse, longitudinal or their combination). By examining the model of the slewing bearing, Kania [10] presented numerical calculations characteristics: deformation - load.

Ricci [18] carried out numerical calculations of distribution of the load among elements of roller bearing. He presented the results of changes in the geometry of the bearing under the specified load. In 2011 Tang et al. [24] developed a numerical roller bearing model using the ANSYS software package. Contact pressure values and maximum contact stresses of elements were calculated. In the same year Laniado-Jacome [13] carried out the research to determine a distribution of the external load on the rolling elements of the rolling bearings loaded with radial force at variable rotational speed. The analysis was performed on a numerical and an analytical model. In Shah Maulik et al. [19] conducted research on the effect of modifying a roller profile on a pressure distribution in contact area. The cylindrical roller bearing durability were investigated using the ANSYS package. Shingala et al. [21] carried out numerical analysis of the contact of rolling elements in needle bearings used in a gearbox. The research which expanded numerical studies on the influence of flows on rolling elements were presented by Deshapande et al. [1] and Shaha Rohit [20].

One of the most widely used programs for numerical calculations is ANSYS. Further work indicates that research carried out using this package is constantly expanding and numerical models are refined. The presented work is an attempt to approximate the numerical model to the geometry and load conditions of actual bearing. The main objective of the research was to assess the effect of radial clearance of roller bearings on phenomena occurring in the contact area rolling elements with raceways. The article presents a methodology of conduct in the determination of subsurface stress necessary to calculate fatigue life by a numerical method.

2. Distribution of external loads

Cylindrical roller bearings are an important element in manufacturing mechanical equipment and are widely used in all sorts of fields. For most applications, cylindrical roller bearings insure a radial load. Cylindrical roller bearing of N or NU type will allow free movement in the axial direction of the shaft in relation to the casing. This allows to overcome the differences in thermal expansion of the materials used in the structure. The NJ type bearings allow to move light axial shaft loads in one direction. Cylindrical roller bearings have a relatively high radial load limits and can operate at high rotational speeds. Their permissible speeds exceed the speed of spherical roller bearings and taper bearings. Rollers in roller bearings are rarely ideal cylinders. In order to reduce stress accumulation at the ends of the roller caused by possible displacement of a shaft and a housing, their ends are rounded and cylinder shapes are corrected. Misalignment of the edge of a bearing, deformation of a shaft, inclination of inner or outer ring may cause tilting the rollers against the rings.

2.1. Distribution of loads in radially-loaded cylindrical roller bearings with radial clearance

The roller bearing consists of two rings (inner and outer) and from a few to several rollers placed between them depending on the size of the bearing. Their even distribution is ensured by the basket. The design of the outer ring of NU type bearing or the inner ring of N type bearing prevents the rollers from moving in the axial direction. In the NJ type bearings, the inner race design allows one-sided displacement

to be achieved with respect to the rollers. Cylindrical roller bearings are made with different radial clearances from C1 to C5. C1 bearings have the smallest radial clearance and C5 the largest. Most of the bearings are produced with normal radial clearance CN. Regardless of that, by selecting the appropriate fit, an initial load in the bearing can be obtained. Then the bearing operates with radial clearance less than zero ($g < 0$). Stribeck [3] demonstrated that the load distribution on rolling bearings with radial force is uneven. Load bearing area for the bearing with positive radial clearance is less than 180°. Figure 1 shows the unloaded bearing with $g = 0$, while Figure 2 shows the bearing loaded with radial force F_r.

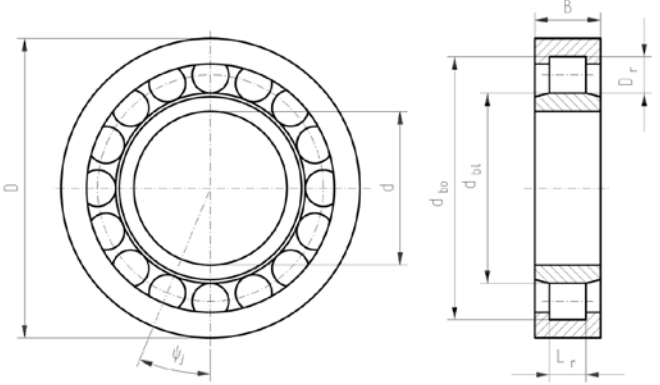

Fig. 1. Bearing with radial clearance g = 0 before loading with force F_r

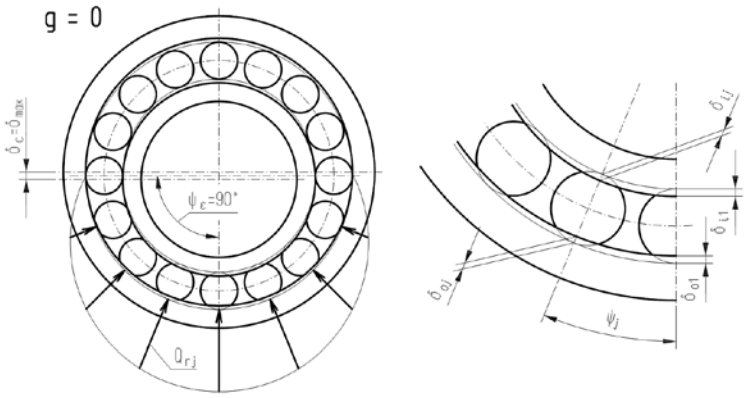

Fig. 2. Bearing with radial clearance g = 0 after loading with force F_r

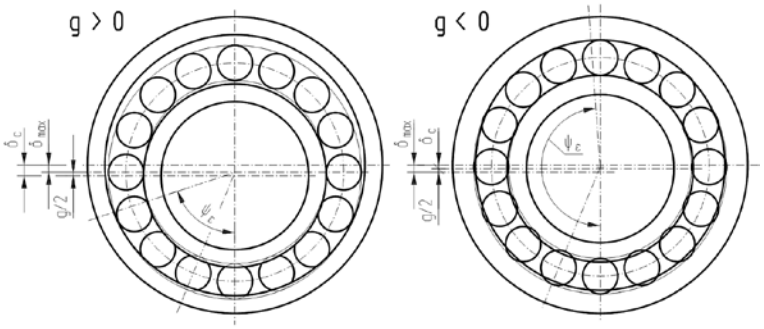

Fig. 3. Bearing with positive and negative radial clearance after loading with force F_r

The number of pairs of rolling elements carrying the load for $g = 0$ can be calculated from this formula:

$$n_{g=0} = INT\left(\frac{Z_r - 1}{4}\right). \quad (1)$$

The number of rolling elements carrying the load in the situations shown in Figure 2 is $2n_{g=0} + 1$. The angle between rolls is calculated from the formula:

$$\psi_j = \frac{2 \cdot \pi}{Z_r} \cdot \quad (2)$$

Figure 3 illustrates the loading bearing zone for positive ($g > 0$) and negative ($g < 0$) radial clearance. The angle of the loaded zone is given by:

$$\psi_\varepsilon = arccos\left(\frac{g}{2 \cdot \delta_c}\right), \quad (3)$$

$$\delta_c = \delta_{max} + g/2 \cdot \quad (4)$$

In the case when $g > 0$, the number of rollers subjected to loading is lower than in the case of $g = 0$. Whereas $g < 0$ it can reach the maximum value equal to the number of rollers in the bearing Z_r.

The equilibrium equation for the bearing loaded with radial force F_r has the form:

$$F_r = Q_{r1} + 2Q_{r2}cos\psi_2 + \ldots + 2Q_{rj}cos\psi_j + \ldots + 2Q_{rn}cos\psi_n \cdot \quad (5)$$

The roller No.1 subjected to the load Q_{r1} cause deformation δ_{max}, that is the sum of contact deformations between the roller and inner ring δ_{i1} and between the roller and outer ring δ_{o1}:

$$\delta_{max} = \delta_{i1} + \delta_{o1} \cdot \quad (6)$$

The value of deformation of the other rollers can be calculated from the formula:

$$\delta_{rj} = \delta_c \cdot cos\psi_j - g/2, \quad (7)$$

where:

$$\delta_{rj} = \delta_{ij} + \delta_{oj} \cdot \quad (8)$$

Knowing the magnitude of deformation, the resultant force Q_{rj} at the contact between the roller and the raceway can be determined according to the Palmgren formula [15, 16]:

$$Q_{rj} = 78000\delta_{i,oj}^{10/9} \cdot l^{8/9}, \quad (9)$$

where the length of the roller-main race contact area is as follows:

$$l = L_r - 2r_c \cdot \quad (10)$$

Equation (5) has been solved numerically using the ROLL1 computer program, built on the basis of the methodology described in the works [25, 26]. The results obtained enable determination of the Stribeck's constant:

$$S_t = Q_{r1} \cdot Z_r / F_r \cdot \quad (11)$$

3. Fatigue life prediction of the radial cylindrical roller bearing

The amount of radial clearance in the radial roller bearing determines the distribution of loads on the rolling elements, and thus has a significant impact on its fatigue life. To determine the fatigue life of the bearing, the methodology described in [25] was applied.

The survival probability of the stationary bearing ring takes the form:

$$ln\frac{1}{\varphi_o} = A \cdot u_o^e L_o^e \int_0^{2\pi} \int_0^l r_{box} \sigma_{oxy}^c Z_{oxy}^{1-h} dx d\psi \ . \quad (12)$$

The survival probability of the bearing ring rotating relative to the load is as follows:

$$ln\frac{1}{\varphi_i} = A \cdot u_i^e L_i^e 2\pi \left[\frac{1}{2\pi} \int_0^{2\pi} \left(\int_0^l r_{bix} \sigma_{ixy}^c Z_{ixy}^{1-h} dx \right)^{1/e} d\psi \right]^e . \quad (13)$$

In the above formulas L is the number of revolutions, u the number of load cycles per one revolution, $\sigma_{x\psi}$ is the maximal von Mises subsurface stresses and $Z_{x\psi}$ is the depth at which these stresses occur (Fig. 4). A is a material constant, which is equal to $4.5 \cdot 10^{-40}$ for the bearing being the object of consideration. The values of the exponents occurring in Eq. (12, 13) are assumed: $c = 31/3$, $h = 7/3$, $e = 9/8$.

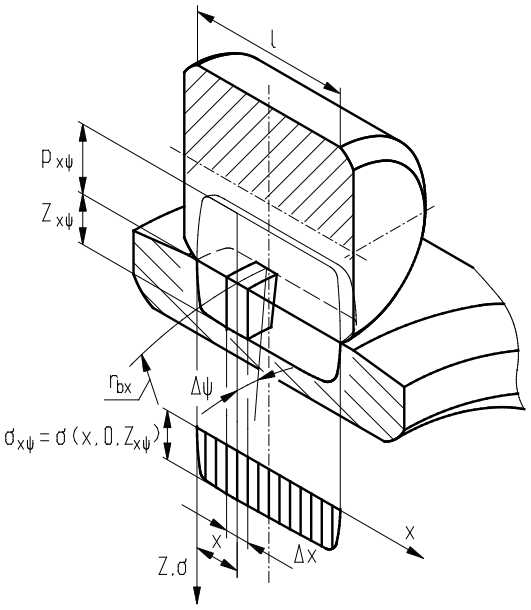

Fig. 4. Distributions of pressure and subsurface stresses deciding on fatigue life of radial cylindrical roller bearing

Using the formula (14), the fatigue life of the tested bearing was determined.

$$L = \left(L_o^{-e} + L_i^{-e} \right)^{-1/e} . \quad (14)$$

For the survival probability $\varphi_o = \varphi_i = 0.9$, the computed value L is identical with the basic rating life L_{10}. The L value is representing number of rotations the bearing can perform before it wears out.

The equations (12) and (13) were resolved by using a program ROLL2 [25]. Determining maximum values substitute subsurface stresses σ in the contact zone between rollers and raceways and estimating the depth Z of their occurrence was necessary to perform the calculations of the fatigue life.

Two methods were used to obtain the distraction of pressure and subsurface stresses:

- "half space" method using the Boussinesq solution describing the deformation of the elastic half-space subjected to pressure – ROLL4 computer program [25, 26];
- finite element method (FEM).

The FEM solid numerical model was developed using the ANSYS – Augmented Lagrange algorithm package. Using the conditions of symmetry, the numerical calculation was done for the half of a roller with raceways, which is shown in Figure 5. The numerical models under investigation were divided into 8-node solid elements of the SOLID185 type and elements which were in contact zone – CONTA174 and TARGE170. Additionally, the symmetry conditions and the degrees of freedom following from real working conditions were considered in the calculations. In order to increase the computational accuracy, a division into elements was increased in the area of the predicted contact and a non-uniform division of contact elements in this area was also applied. The distance between the mesh nodes of the contact area elements of the roller is 0.05 mm (with bearing diameter 15 mm). The distances between the node of the remaining raceways and the roller are adjusted at an angle eliminating component shape errors. As a result, the numerical model contains 200363 nodes in 88910 elements. Considering the character of the contact of a roller bearing with the raceways, the roller was treated as a contact surface. Raceways surfaces were assumed as target surfaces. The displacement towards every axis of the coordinate system for the outer surface of the ring was blocked. The inner ring was allowed to move only in the direction of the "z" axis. The coefficient of stiffness of FKN = 1.5 has been adopted. Using the symmetry conditions, the model was loaded with force $F_r / 2$.

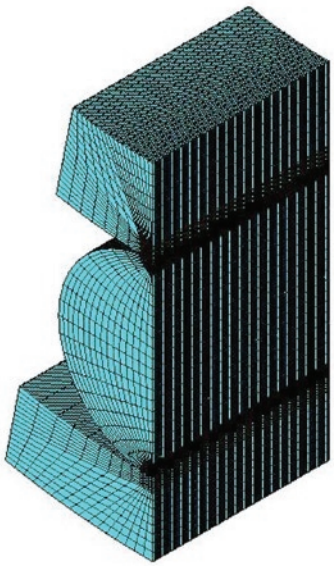

Fig. 5. FEM numerical model grid of the roller-raceways contact

4. Subject of study

The subject of study was the NU 213 ECP cylindrical roller bearing [22]. Parameters of the tested bearing are shown in Table 1.

The rollers were corrected according to the modified logarithmic correction proposed by Krzemiński-Freda [11]. The generator profile was the same as described in the paper [26] (Fig. 6). Parameters of the logarithmic correction profile of NJ 213 ECP bearing are not published by the manufacturer.

Table 1. Parameters of the NU 213 ECP cylindrical roller bearing [22]

Bearing bore diameter	d = 65 mm
Bearing outside diameter	D = 120 mm
Bearing width	B = 23 mm
Diameter of the outer ring raceway	d_{bo} = 108.5 mm
Diameter of the inner ring raceway	d_{bi} = 78.5 mm
Roller diameter	D_r = 15 mm
Roller length	L_r = 15 mm
Roller chamfer	r_c = 0.5 mm
Number of rollers in the bearing	Z_r = 16
Dynamic load rating	C = 122000 N

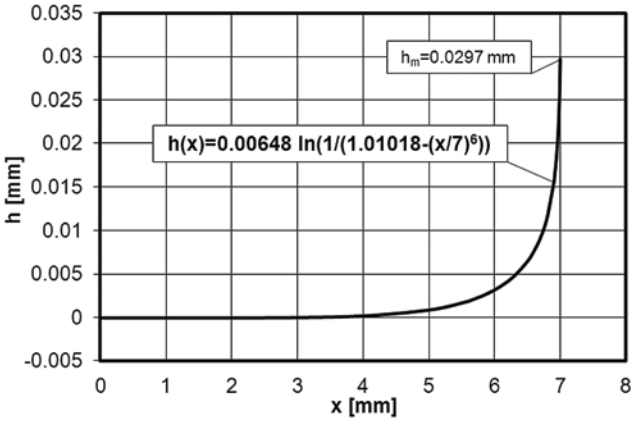

Fig. 6. Roller generator profile with a modified logarithmic correction [26]

5. Results

5.1. Rollers load

According to Krzemiński-Freda [12] cylindrical roller bearings loaded with radial force $F_r = 0.3\ C$ operate under hard operating conditions. Normal operating conditions are considered to be such that the load is: $F_r = (0.07–0.12)\ C$. The researched bearing was loaded with the force: $F_r = 0.3\ C = 36600$ N and $F_r = 0.1\ C = 12200$ N. Table 2 shows load distributions calculated with ROLL1 computer program for selected radial clearances. Figure 7 illustrates the distributions of radial load Q_r on the rollers for $F_r = 0.3\ C$.

Table 2. Radial load distributions on NU 213 ECP bearing rollers

		F_r = 36600 N				
g [mm]		-0.038	-0.019	0.0	0.019	0.038
ψ_ε [°]		180.0	113.36	90.00	78.49	71.32
Roller No.	ψ_j [°]	Q_{rj} [N]	Q_{rj} [N]	Q_{rj} [N]	Q_{rj} [N]	Q_{rj} [N]
1	0	9447	8672	9342	10015	10673
2	22.5	9069	8148	8556	8962	9353
3	45	8001	6676	6357	6036	5706
4	67.5	6429	4535	3213	1944	752
5	90	4624	2141	0	0	0
6	112.5	2888	51	0	0	0
7	135	1495	0	0	0	0
8	157.5	631	0	0	0	0
9	180	349	0	0	0	0
S_t		4.13	3.79	4.08	4.38	4.67
		F_r = 12200 N				
g [mm]		-0.019	-0.0095	0.0	0.019	0.038
ψ_ε [°]		180.00	128.45	90.00	67.71	58.07
Roller No.	ψ_j [°]	Q_{rj} [N]	Q_{rj} [N]	Q_{rj} [N]	Q_{rj} [N]	Q_{rj} [N]
1	0	3721	2875	3114	3701	4067
2	22.5	3598	2725	2852	3201	3344
3	45	3250	2304	2119	1821	1381
4	67.5	2735	1688	1071	12	0
5	90	2141	991	0	0	0
6	112.5	1562	343	0	0	0
7	135	1088	0	0	0	0
8	157.5	782	0	0	0	0
9	180	678	0	0	0	0
S_t		4.88	3.77	4.08	4.85	5.33

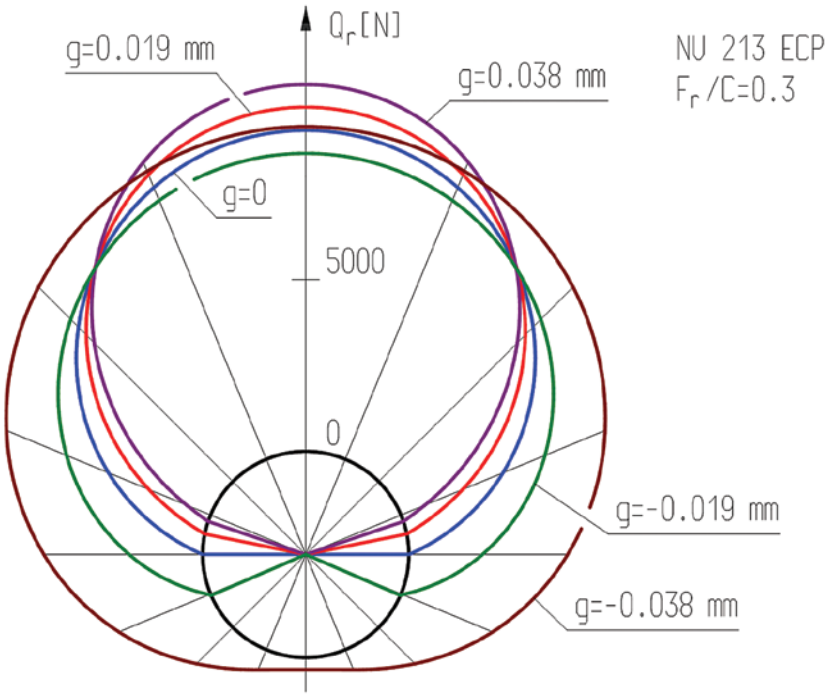

Fig. 7. The distributions of radial load on the rollers of NU 213 ECP bearing

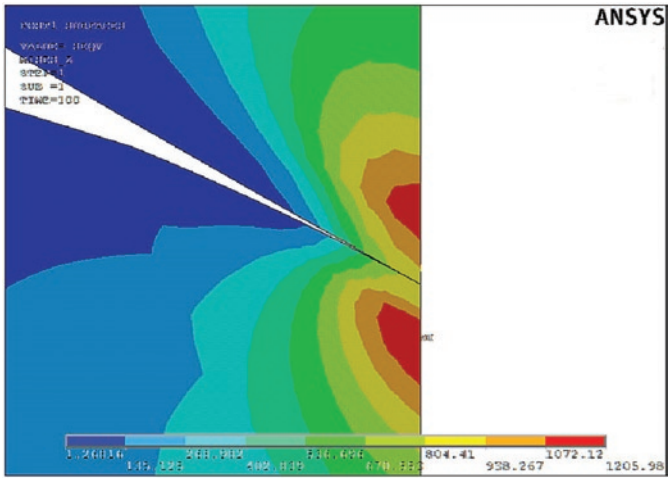

Fig. 8. Distributions of von Mises stresses below the roller-inner ring raceway contact surface

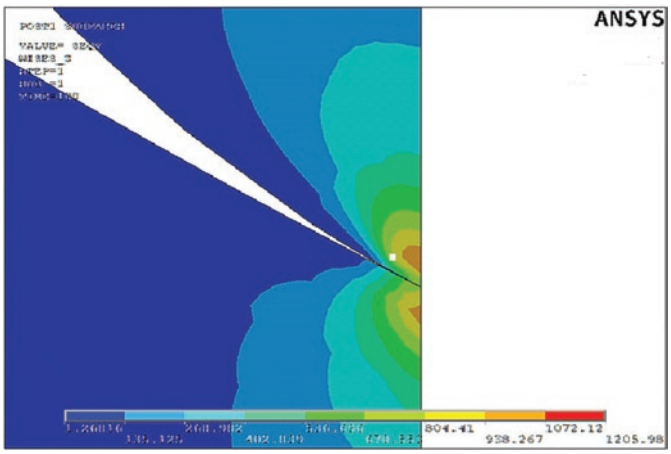

Fig. 9. Distributions of von Mises stresses below the roller-outer ring raceway contact surface

5.2. Surface pressure and von Mises stress distributions

As a result of numerical calculations, data necessary to analysis the phenomena occurring in the contact zone of the kinematic pair of the researched model were obtained. The obtained results of the bearing calculations NU 213 ECP are shown in the form of graphs and maps. The researched bearing is loaded with radial force F_r = 36600 N assuming that the axes of the rolling elements and the raceways of the bearing are parallel, the radial clearance is g = 0.038 mm. For the calculations of surface pressures and von Mises stresses with the "half space" method, it was assumed that bearing elements were made of elastic-ideally plastic material. The material properties were determined by Young's modulus E = 208 GPa, Poisson's constant ν = 0.3 and the tensile yield strength σ_o = 1950 MPa. The same assumptions as regards the material characteristics were made during the calculations of surface pressures and von Mises stresses with the FEM.

Figure 8 shows a graphical map of the distribution of maximum von Mises stress below the surface of the roller-inner ring raceway contact.

Figure 9 shows the distribution of maximum von Mises stress below the surface of the roller-outer race contact. Figures 10 and 11 show the contact surface of the roller with the inner and outer ring raceway with detail.

In the basic version, ANSYS gave only one maximum value and one minimum von Mises stress value and coordinates *(x, z)* of the place of occurrence of these stresses across the contact area. In this paper, the authors present the possibility of defining the von Mises stress distribution in a cross-section determined by any x-coordinate, which makes it possible to determine maximal values of stresses σ and the depth of their occurrence Z in the cross-section. The ANSYS package allows direct determination of the von Mises stress distribution in the plane selected by the user. Example of calculation results are presented in Figure 12, 13 and 14. The results obtained with this method enabled determination of the maximum von Mises stress dis-

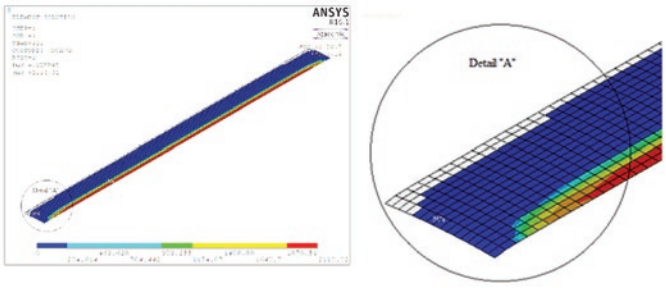

Fig. 10. Contact surface of the roller with the inner ring raceway

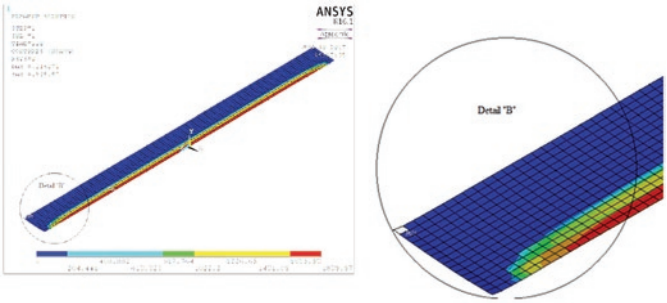

Fig. 11. Contact surface of the roller with the outer ring raceway

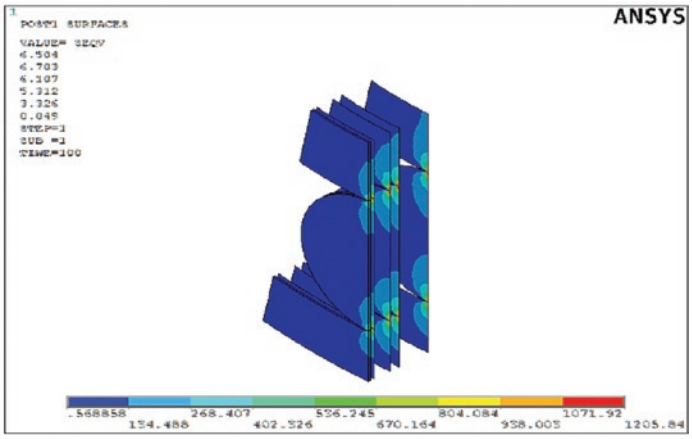

Fig. 12. The example values of von Mises stresses at the material depth

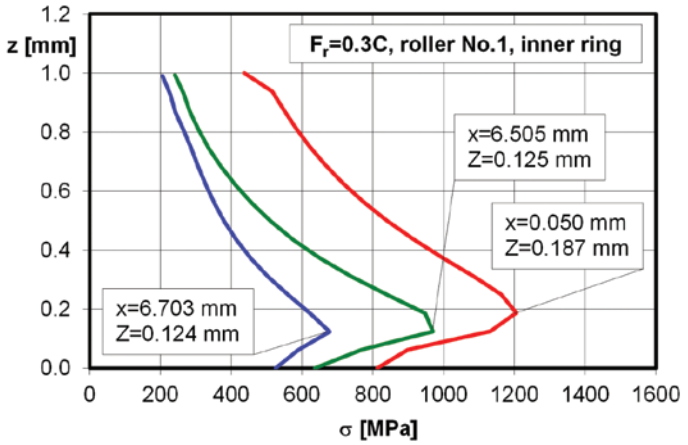

Fig. 13. Distribution of von Mises stresses in the three example cross-sections of the roller-inner ring raceway contact

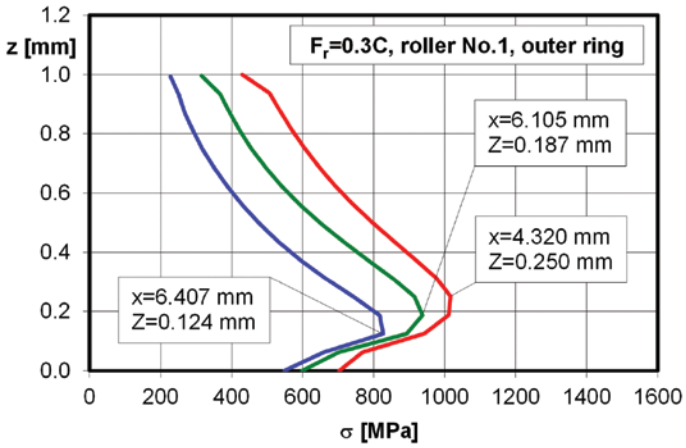

Fig. 14. Distribution of von Mises stresses in the three example cross-sections of the roller-outer ring raceway contact

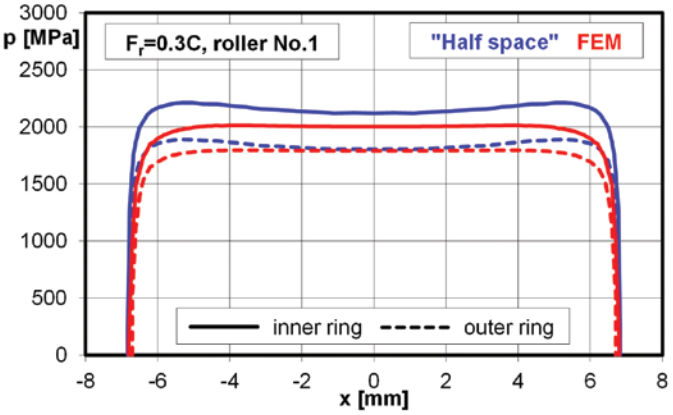

Fig. 15. Surface pressure distributions along the x axis of the most heavily loaded roller in contact with the inner and outer ring raceway

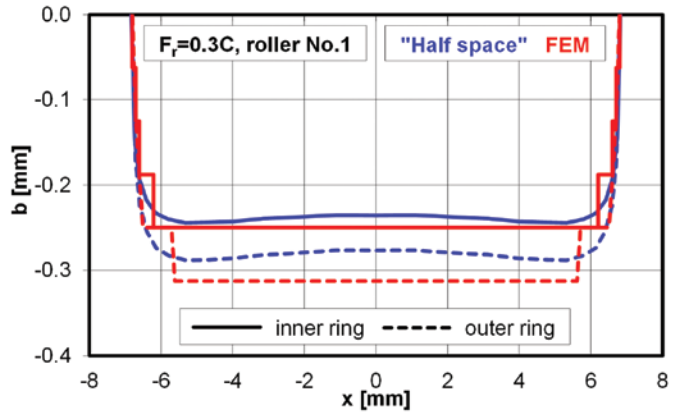

Fig. 16. Contact areas of a roller with raceways

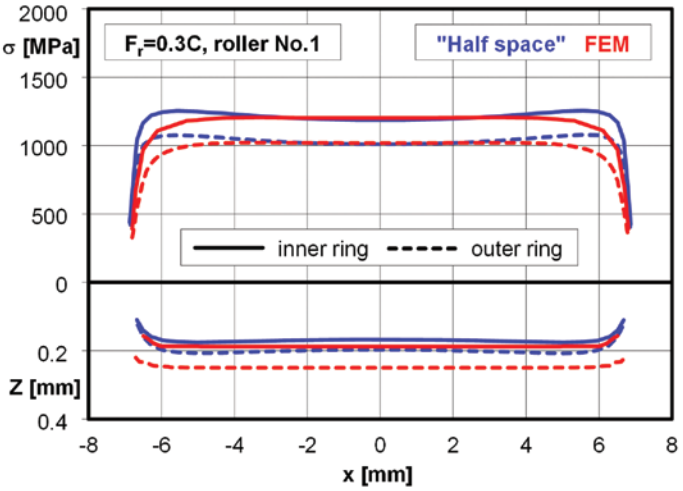

Fig. 17. Distributions of maximal von Mises stresses σ and the depth of their occurrence Z in the most heavily loaded roller in contact with the inner and outer ring raceway

tributions and the depth of their occurrence along the contact line. These distributions are necessary to determine the expected fatigue life of the bearing.

In Figure 15 a comparison of distributions of maximal surface stresses along the *x* axis of the most loaded roller (No. 1) in contact with the inner and outer ring raceway, obtained with ROLL4 (”half space” method) and with the FEM is presented. Figure 16 shows boundaries of the contact area of a roller with both raceways.

The results obtained using elastic “half space” solution and FEM are sufficiently convergent. The shape and size of the contact zones are similar. The only difference in the surface stresses distributions is only observed near the ends of the contact field. This is due to the small surface pressure exerted on this points and has a little effect on the estimations of fatigue life.

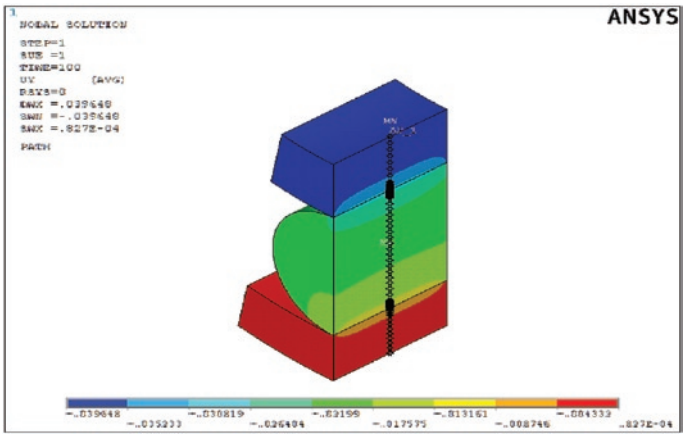

Fig. 18. Displacement of radial cylindrical roller bearing elements

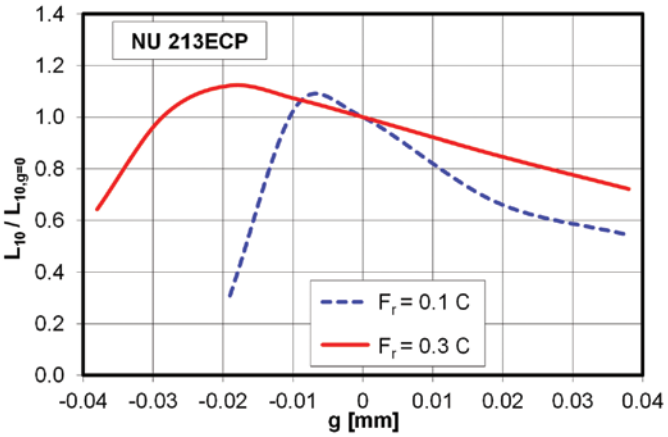

Fig. 20. Relative bearing life as a function of radial clearance

Figure 17 shows the stresses σ and the depths *Z* of the most heavily loaded roller in contact with the inner and outer ring raceway, obtained with both method.

The curves describing the depth at which the maximal von Mises stresses occur, determined by both the „half space" method and by FEM, have a shape similar to the von Mises stress distributions. The distributions of the depth *Z* determined with the FEM are characterized by slightly higher values if compared to the plots obtained with the "half space" method. These differences are due to the model used in the FEM which, in contrast to the "half space" method, simultaneously considers the contact of the roller with an inner and an outer ring.

The ANSYS program also allows to get a map of the displacements inside the contacting bodies. Figures 18 and 19 show the displacement of cooperating bearing elements due to the applied load. Figure 19 shows that the largest displacement is near the contact between the roller and raceways.

5.3. Fatigue life

Due to the long time necessary to solve the contact problem using FEM, only the distributions obtained using the "half space" method were used to calculate the expected fatigue life of the bearing.

In Figure 20, as a function of radial clearance, the characteristics of bearing fatigue life changes with respect to fatigue life for radial clearance equal to zero are presented. The course of the curves is a confirmation of the known fact that the bearing achieves the highest durability with a little radial interference [12].

In case of radial load F_r = 0.3 *C*, the fatigue life of the tested bearing achieves the highest values (i.e. greater than the durability for g = 0) when radial clearances is between the range from g = 0 to

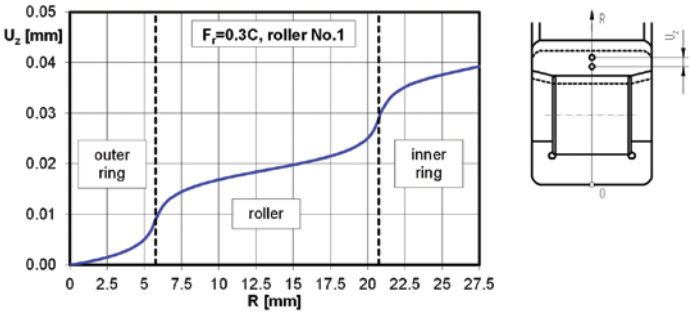

Fig. 19. Local displacement Uz inside the bearing elements

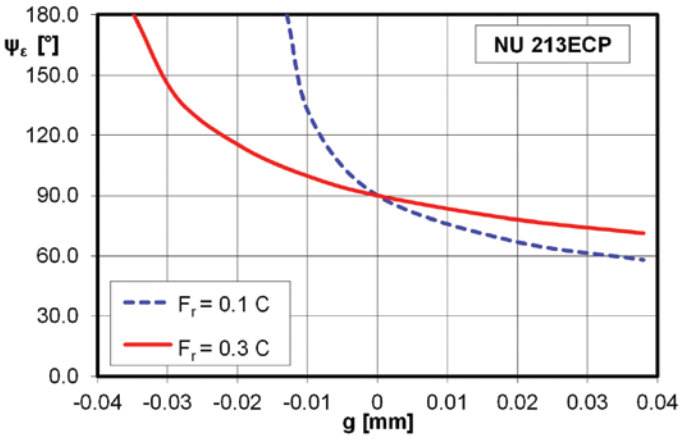

Fig. 21. Angle of the loaded zone as a function of radial clearance

g = –0.029 mm. In the case of radial load F_r = 0.1 *C*, the highest fatigue life is achieved by the bearing with radial clearances in the range from g = 0 to g = –0.011 mm. In both cases, this corresponds to the angles of the loaded zone in the range of $90° \le \psi_\varepsilon \le 140°$ (Fig. 21).

The greatest increase in fatigue life in relation to fatigue life for zero radial clearance that can reach the bearing is equal to $L_{10} / L_{10,g=0} \approx 1.1$. This increase occurs at the angle $\psi_\varepsilon \approx 115°$, regardless of the radial load value. However, as the load increases, the amount of interference increases, at which the greatest increase in fatigue life is achieved. In case of radial clearances greater than zero and for interferences with values greater than the values given above, the fatigue life of the tested cylindrical roller bearing is less than the fatigue life for clearance g = 0. The reasons for this phenomenon are explained in Figure 7, presenting the load distributions for various radial clearances. As shown, in the range of clearance from g = 0 to g = –0.029 mm, the number of rollers subjected to the load is greater than in the case of radial clearance $g > 0$, but at the same time the values of forces acting on the most loaded rollers that determine the bearing fatigue life are lower. For radial clearances smaller than g = –0.029 mm and greater than g = 0 both the force values increase, which results in a decrease in fatigue life.

6. Conclusions

The applied methodology allows to predict the durability of any radial cylindrical roller bearing for a given load and radial clearance by introducing parameters into the calculations that could not be taken into consideration when doing the analytical computations. One of them is the correction of roller generators.

The methodology enabled to determine the distributions of radial load on the rolling elements at a predetermined radial clearance. It also allows to calculate the Stribeck's constant.

As a result of numerical calculations, the data necessary to analysis the phenomena occurring in the contact zone of the kinematic pair of the researched model were obtained. In case of testing of rolling bearings, it was necessary to build complex solid models of cooperating elements. Knowledge of subsurface stress distributions is necessary to determine the fatigue life of rolling bearings.

FEM allowed to estimate accurate results on the state of subsurface stresses. Similar outcome can be obtained by solving the Boussinesq problem for elastic half-space.

The ANSYS package allows to determine the von Mises stress distribution in the plane selected by the user. The possibility of defining the von Mises stress distribution in the section defined by any x coordinate is particularly important for predicting the fatigue life of radial cylindrical bearings subjected to a complex load. The complex load causes a significant tilting of the rolling elements of the bearing, which requires knowledge of the exact position of the maximum stress in the material.

The performed analyses showed that the radial cylindrical roller bearing achieves the highest durability with a little radial interference. The greatest increase in fatigue life in relation to fatigue life for zero radial clearance the bearing achieves for a radial interference at which the angle of the loaded zone is equal to $\psi_\varepsilon \approx 115°$, regardless of the radial load value. The increase in fatigue life in this case is equal to $L_{10} / L_{10,g=0} \approx 1.1$.

References

1. Deshpande H, Kulkarni S, Gandhare B S. Investigation on effect of defect on cylindrical roller bearing, by experimental and FEA approach. Iternational Journal of Emerging Technology and Advanced Engineering 2014; 4 (6).
2. Hamrock B J, Anderson W J. Rolling-element bearings. NASA RP_1105/REV1; 1983.
3. Harris T A. Rolling bearing analysis. Wiley-Interscience, New York, USA; 1991.
4. Harris T A, Kotzalas M N. Advanced concepts of bearing technology. Rolling bearing analysis. Fifth edition. CRC Press; 2006, https://doi.org/10.1201/9781420006582.
5. Harris T A, Kotzalas M N. Essential concepts of bearing technology. Fifth edition. CRC Press; 2006.
6. Harris T A, Kotzalas M N. Rolling Bearing Analysis. Fifth Edition - 2 Volume Set. CRC Press; 2007.
7. Hertz H. Uber die Beruhrung fester elastischer Korper. Gesammelte Werke (P. Lenard, ed.), Bd. 1, (J.A. Barth, Leipzig; 1895):155-173.
8. Jones A. A general theory for elastically constrained ball and roller bearing under arbitrary load and speedy conditions. Trans ASME 1960; 105: 591-595.
9. Jonson K L. Contact mechanics. Cambrige University Press, Cambrige; 1985, https://doi.org/10.1017/CBO9781139171731.
10. Kania L. Modelling of rollers in calculation of slewing bearing with the use finite elements. Mech Mach Theory 2006; 41: 1359-1376, https://doi.org/10.1016/j.mechmachtheory.2005.12.007.
11. Krzemiński-Freda H. Correction of the generators of the main working surfaces of roller bearings. Arch Mech Eng 1990; 37: 115–132.
12. Krzemiński-Freda H. Roller Bearing. PWN, Warsaw; 1985 (in polish).
13. Laniado-Jacome E. Numerical model to study of contact force in a cylindrical roller bearing with technical mechanical event simulation. J Mech Eng Autom 2011; 1: 1–7.
14. Lundberg G. Cylinder compressed between two plane bodies. SKF Reg. 4134 1949.
15. Lundberg G, Palmgren A. Dynamic capacity of rolling bearings. Acta Polytech Scand Mech Eng 1947; 1(3): 1-52.
16. Lundberg G, Palmgren A. Dynamic capacity of roller bearings. Acta Polytech Scand Mech Eng 1952; 2(4): 96-127.
17. Palmgren A. Ball and roller bearing engineering. Third ed., SKF Industries, Philadelphia, PA 1959.
18. Ricci M C. Internal loading distribution in statically loaded ball bearings subjected to a centric thrust load: alternative approach. World Academy of Science, Engineering and Technology 2010; 65: 641-649.
19. Shah Maulik J, Darji P H. Fatigue life improvement through reduction of edge pressure in cylindrical roller bearing using FE analysis. International Journal For Technological Research in Engineering 2014; 1(10): 1069-1074.
20. Shaha Rohit D, Kulkarni S S. Vibration analysis of deep groove ball bearing using finite element analysis. International Journal of Engineering Research and Applications 2015; 5(5): 44-50.
21. Shingala Niraj R, Sata Ankit V, Delvadiya Parth V, et al. Contact stress analysis of needle roller bearing used in synchromesh gear box. Trends in Machine Design 2018; 5(1): 5–20.
22. SKF General Catalogue; 2007.
23. Stribeck R. Ball bearings for various loads. Reports from the Central Laboratory for Scientific Technical Investigation, translation by K.W. Van Treuren et al., Trans ASME 1907; 29: 420-463.
24. Tang Zhaoping, Sun Jianping. The contact analysis for deep groove ball bearing based on Ansys. Procedia Engineering 2011; 23: 423-428, https://doi.org/10.1016/j.proeng.2011.11.2524.
25. Warda B, Chudzik A. Fatigue life prediction of the radial roller bearing with the correction of roller generators. International Journal of Mechanical Science 2014; 89: 299-310, https://doi.org/10.1016/j.ijmecsci.2014.09.015.
26. Warda B, Chudzik A. Effect of ring misalignment on the fatigue life of the radial cylindrical roller bearing. International Journal of Mechanical Science 2016; 111-112, https://doi.org/10.1016/j.ijmecsci.2016.03.019.

Agnieszka CHUDZIK
Department of Dynamics
Lodz University of Technology
Stefanowskiego 1/15, 90-537 Lodz, Poland

Bogdan WARDA
Department of Vehicles and Fundamentals of Machine Design
Lodz University of Technology
Stefanowskiego 1/15, 90-537 Lodz, Poland

E-mails: Agnieszka.Chudzik@p.lodz.pl, Bogdan.Warda@p.lodz.pl